Bioconjugation of Electron-Probe Au_{25} Nanocluster to Monoclonal Antibody

Katarzyna Joanna Malawska,[1] Shinjiro Takano,[2] Kounosuke Oisaki,[1,*] Haruaki Yanagisawa,[3] Masahide Kikkawa,[3] Tatsuya Tsukuda,[2] and Motomu Kanai[1,*]

[1]Graduate School of Pharmaceutical Sciences, The University of Tokyo, 7-3-1 Hongo, Bunkyo-ku, Tokyo 113-0033, Japan

[2]Graduate School of Science, The University of Tokyo, 7-3-1 Hongo, Bunkyo-ku, Tokyo 113-0033, Japan

[3]Department of Cell Biology and Anatomy, Graduate School of Medicine, The University of Tokyo, 7-3-1 Hongo, Bunkyo-ku, Tokyo 113-0033, Japan

KEYWORDS: bioconjugation, tryptophan, gold nanocluster, antibody conjugate, immunogold labeling, cryogenic electron microscopy (Cryo-EM)

ABSTRACT: We report the first bioconjugation of Au_{25} nanocluster to a monoclonal antibody without protein engineering, in a step toward the development of high-resolution probes for cryogenic electron microscopy (cryo-EM) and tomography (cryo-ET). To achieve this, we improved the tryptophan (Trp)-selective bioconjugation step by using easy-to-analyze hydroxylamine (ABNOH) reagents in a pH-neutral buffer, instead of using N-oxyl radicals (ABNO) under acidic conditions as previously developed. This new protocol allowed for the application of Trp-selective bioconjugation to acid-sensitive proteins such as antibodies. We found that a two-step procedure, utilizing first Trp-selective bioconjugation for homogeneous introduction of azide groups to the protein and then strain-promoted azide-alkyne cycloaddition (SPAAC) to attach bicyclononyne (BCN)-presenting, redox-sensitive Au_{25} nanocluster, was key to successful immunogold synthesis. This procedure is scalable. The covalent labeling of the antibody with gold nanoclusters was confirmed by various analytical methods, including cryo-EM analysis of the Au_{25} nanocluster conjugates. In comparison with a non-homogenous variant prepared by lysine-selective bioconjugation, Trp-selective conjugates exhibited both satisfactory gold cluster modification and minimal loss of antigen-binding ability.

INTRODUCTION

Cryogenic electron microscopy (cryo-EM) and tomography (cryo-ET) are indispensable modern tools for structural biology. A low signal-to-noise ratio nevertheless hinders the technology despite significant advances in sample vitrification, direct electron detectors, and software designed for single particle analysis, etc.[1–3] One solution would be to label protein specimens with heavy metal particles, which aid diffraction of the electron beam. Labeling with gold nanoparticles has been studied due to the attractive properties of gold. Despite being a heavy metal, gold is not toxic to cells or living organisms and can easily form particles of various sizes.[4] In 1971, Faulk and Taylor published the first electron-probing of biomolecules using antibody-gold nanoparticle conjugates (*immunogold labeling*; Figure 1a).[5] This pioneering work successfully visualized immuno-aggregates of bacteria by conventional electron microscopy. Preparation of the electron probe, however, relied on non-specific physisorption of antibodies onto non-homogenous, structurally undefined colloidal gold. The weak electrostatic interaction between proteins and gold nanoparticles that results from physisorption can be easily abolished and is one of its intrinsic drawbacks.[6] Liberated gold nanoparticles may non-specifically label other proteins, often causing false-positive and non-precise imaging results. Although physisorption-based antibody-gold conjugates remain in use, the only successful application is for visualizing the macroscopic distribution of antigens on the cell surface.

Site-selective covalent bioconjugation and gold particle size are two crucial factors for high-resolution immunogold labeling.[4,6] Because the covalent bond-formation between gold and thiols is the basis for gold nanoparticle formation,[7] targeting cysteine (Cys) residues to achieve bioconjugation is a logical strategy. However, on-demand installation of unpaired Cys frequently requires genetic manipulation, which makes expression of large proteins such as antibodies challenging.[6,8,9] Another commonly used bioconjugation targeting lysine (Lys) residues produces non-homogenous

conjugates and sometimes affects inherent protein functions, though modern site-selective techniques are intensively studied.[10,11] Francis and co-workers developed a novel bioconjugation method that involves the enzymatic oxidation of phenols on the surface of gold nanoparticles.[12] The reported protocol was applicable to proteins containing unpaired Cys residues or *N*-terminal prolines, as well as thiol-modified DNA strands. However, only large gold nanoparticles with a diameter of approximately 5 nm were employed in this study.

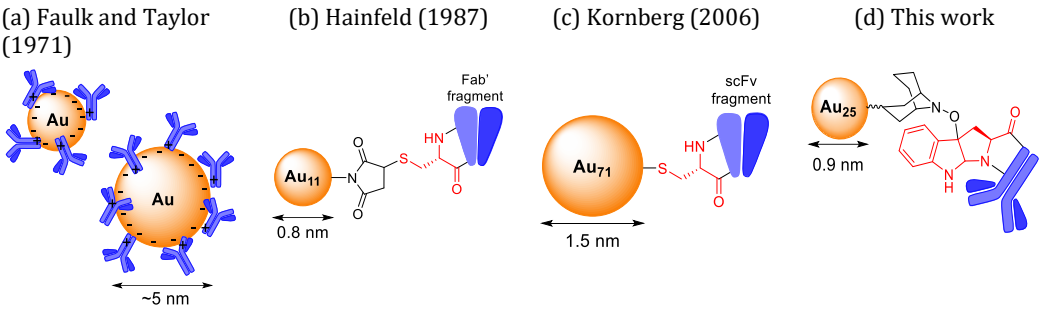

	(a) Faulk and Taylor (1971)	(b) Hainfeld (1987)	(c) Kornberg (2006)	(d) This work
Atomically defined?	×	√	√	√
Stable linkage?	×	√	√	√
Homogenous?	×	√	√	√
Subnanometer-size cluster	×	√	×	√
No genetic manipulation?	√	√	×	√
No Ag^+ enhancement?	√	×	√	√

Figure 1. Comparison of immunogold labeling strategies.

As for the size of the particle, smaller gold particles have a potential advantage in high-resolution cryo-EM. Artefacts introduced by the probe are less likely in cryo-EM/ET observations due to its small size. However, small gold nanoparticles (< 2 nm) easily aggregate, and tissue penetration of the resulting colloidal gold conjugates is often problematic.[4,6,13] *Gold nanoclusters* have been investigated as a novel class of particles since the 1980s. They are composed of core gold atoms with atomically defined alignments and discrete numbers. The number of gold atoms in the core and surrounding ligand structures is closely correlated with their molecule-like character. They are excellent candidates for precise gold labeling due to high stability against aggregation, small core size (~ 1 nm), and possible implantation of biocompatible thiol ligands. One of the first cluster-based reagents for electron microscopy was undecagold, containing 11 Au atoms ligated by an amine-functionalized phosphine, reported by Bartlett in 1978.[14] In 1987, Hainfeld used undecagold ligated by a maleimide-functionalized phosphine to label the Fab fragment of an antibody to horse ferritin through Cys conjugation (Figure 1b). The binding affinity of the probe towards ferritin was retained, and the resolution of scanning transmission electron microscopy (STEM) images was successfully improved.[15] High-resolution structural studies of several other proteins were also reported.[16–19] However, due to the ultra-small size of the core, a silver enhancement to visualize the objects in standard transmission electron microscopy (TEM) is sometimes required.

Site-selective conjugation of larger gold nanoclusters such as Au_{71} (Figure 1c),[20] Au_{144},[21] or Au_{102}[22–24] to proteins was reported, but it required protein engineering to introduce additional Cys residues. Moreover, high concentrations of clusters and proteins at an elevated temperature were required to facilitate conjugation through the thiol exchange reaction.[22] Such conditions may not be suitable for whole antibodies, which aggregate easily.

Au_{25} nanocluster, with a small, atomically defined gold core (~ 0.9 nm), exhibits high chemical stability.[25] Applying suitable thiol ligands, $Au_{25}SR_{18}$ can be synthesized as a biocompatible and water-soluble nanoparticle. Various biorelevant ligands, including tiopronin,[26] cysteine,[27] glutathione,[28] and even proteins such as bovine serum albumin (BSA),[29] have been successfully used. Importantly, the nanocluster can be visualized by ACTEM (aberration-corrected TEM) without silver enhancement.[30] Rovira and coworkers[31] conducted theoretical studies on the mechanism for labeling an antibody fragment (scFv) with Au_{25}(glutathione)$_{18}$ via a ligand exchange reaction. However, any practical approach for the

site-selective conjugation of Au_{25} nanoclusters to proteins has not yet been reported.

In this report, we present the conjugation of Au_{25} nanoclusters to a monoclonal antibody by tryptophan (Trp)-selective bioconjugation, producing highly homogeneous gold-antibody conjugates (Figure 1d). Conjugates prepared by this method are compared with conjugates prepared by conventional, non-homogenous Lys-selective bioconjugation using cryo-EM.

RESULTS

Improvement of Trp-selective bioconjugation for pH- and redox-sensitive proteins/payloads. Trp-selective bioconjugation has intrinsic advantages over other methods targeting nucleophilic residues such as Lys or Cys. The abundance and exposure of Trp within proteins are among the smallest of all the proteogenic amino acids, yet most proteins contain at least one Trp residue.[32,33] Targeting rarely exposed Trp, therefore, improves site-selectivity and narrows labeling distribution, producing homogenous conjugates. This is especially crucial when modifying antibodies.[10] In 2016, we reported a Trp-selective bioconjugation of peptides and proteins using a 9-azabicyclo[3.3.1]nonan-3-one-derived radical, keto-ABNO (**1**: Figure 2a).[34] We further demonstrated that this method was useful in generating a folate-conjugated humanized monoclonal antibody without significant loss of its biochemical functions *in vitro*.[35,36]

We still needed an improved protocol, however, for application of this method to complex proteins (such as antibodies) and pH- and redox-sensitive payloads (Au_{25} clusters). In the original protocol, we employed a NO_x oxidant to generate the conjugation-active oxoammonium species, keto-ABNO$^+$ **2**, from **1** through single-electron oxidation (Figure 2a).[34] For the generation of NO_x species from $NaNO_2$, however, the protocol required weakly acidic media (pH ~3) that might affect pH-sensitive proteins/payloads. Moreover, NO_x species generated in situ might produce nitrosylated byproducts. We developed a NO_x-free protocol using electrochemical oxidation of **1** in neutral aqueous media; however, over-oxidation was a problematic side reaction (Figure 2b).[37]

To improve the protocol, we used a hydroxylamine reagent, keto-ABNOH **3**, rather than radical **1**. Compound **3** is more stable, and thus more storable, than **1**. Furthermore, it is possible to precisely assess the purity of **3** and its derivatives by NMR. As was partly expected, however, a more reactive and selective oxidant was necessary to activate **3** to **2**. During mechanistic studies in the electrochemical method (Figure 2b), we found that TEMPO$^+$, generated through anodic oxidation of a TEMPO additive, accelerated the reaction as an electrochemical mediator.[37] Thus, we screened various oxidants and identified an isolable oxoammonium salt, TEMPO$^+$•BF_4^- **4**,[38,39] as a novel activator for **3**. This protocol was applicable in aqueous, buffered media under neutral pH conditions (Figure 2c). Potentially oxidation-sensitive amino acids, such as Ser, Lys, Tyr, and His were not affected (Figures S1-S8), indicating that **4** acted as a selective oxidant to **3**.

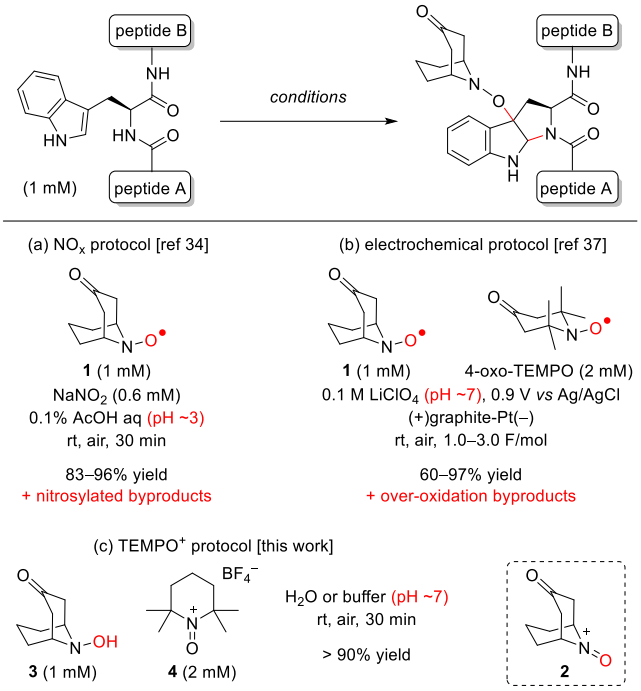

Figure 2. Improvement of Trp-selective bioconjugation protocol.

Trp-selective bioconjugation of Au_{25} nanoclusters with trastuzumab. The most straightforward approach for the synthesis of Au_{25}-protein conjugates is direct Trp-conjugation using keto-ABNOH-grafted Au_{25} nanocluster **6** (Figure 3a). Thus, we synthesized **6** through a thiol exchange reaction between water-soluble $Au_{25}(SCH_2CH_2NH_2)_{18}$ and 1.3 equiv HS-PEG_4-ABNOH **5** (Murray place exchange reaction).[40,41] Electrospray ionization mass spectrometric (ESI-MS) measurements of **6** indicated that 2–3 ligands were exchanged to **5** on the surface of Au_{25} nanocluster. **6** was freely soluble in H_2O. Then, we conducted bioconjugation of trastuzumab with **6** (20 equiv) in the presence of **4** (30 equiv) in a buffer (Figure 3a). Monitoring the reaction progress by liquid chromatography-electron spray ionization (ESI) mass spectroscopy (LC-MS) indicated, however, that the reaction proceeded only minimally. Even when detected, the Au_{25} conjugate was only observed in traces of its

oxidized form. Further optimization to increase the yield was not successful.

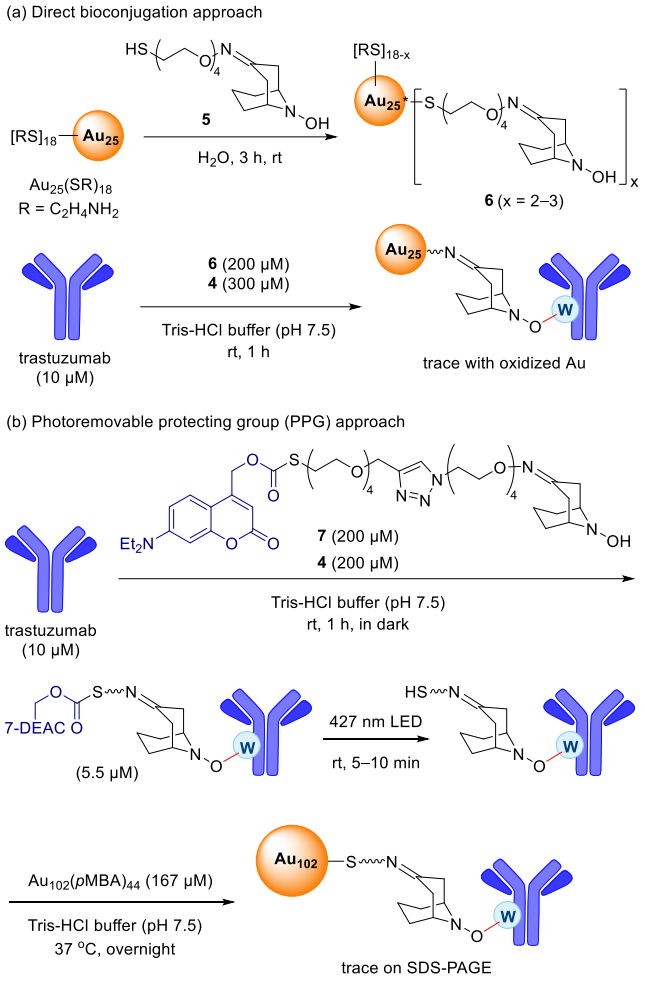

Figure 3. Unsuccessful approaches for the synthesis of Au_{25} nanocluster-trastuzumab bioconjugates at Trp.

Thus, we separated the Au_{25} labeling step from the oxidatively promoted Trp-selective bioconjugation step (Figure 3b). In this approach, the protein was first conjugated with a keto-ABNOH derivative bearing a photoremovable protecting group (PPG)-masked thiol[42] (PPG-S-linker-ABNOH). After photoirradiation to reveal the free thiol, the gold cluster was added to the label through the thiol exchange reaction. We explored several PPG for thiols,[43] including *o*-nitroveratryl (*o*Nv), 7-diethylaminocoumarin oxycarbonyl (7DEAC), and *p*-hydroxyphenacyl (*p*HP) groups.[44] Because detection of the Au_{25}-conjugated protein was difficult, we optimized the reaction using a larger cluster, Au_{102}(*p*MBA)$_{44}$ (*p*MBA = *p*-methoxybenzoic acid),[22] which was easily visible in SDS-PAGE. 7DEAC-containing **7** afforded the best results; however, the conjugate was produced in only trace yield at best (Figure S16).

Therefore, we attempted the third approach involving Trp-selective bioconjugation with azide-containing keto-ABNOH **8**,[35] followed by strain-promoted azide-alkyne cycloaddition (SPAAC)[45,46] for the attachment of Au_{25} nanocluster (Figure 4). SPAAC is more appropriate for the second step than the copper-promoted click reaction because copper ions may affect the properties of Au_{25} nanoclusters.[47] We synthesized Au_{25}-BCN **9** from Au_{25}(captopril)$_{18}$ **10**[48] through amide formation with amine-containing BCN **11** (Figure 4a). ESI-MS studies indicated that **9** contained primarily one BCN moiety on the surface. Meanwhile, Trp-bioconjugation of **8** with trastuzumab proceeded under buffered conditions (pH 6.8) for 1 h. The slightly acidic conditions were beneficial in this initial step to minimize aggregation of pH-sensitive trastuzumab. After quenching oxidants with sodium ascorbate (NaAsc) and performing ultrafiltration to eliminate small molecules, conjugate **12** was obtained in high yield (Figure 4b), as was indicated by SEC-HPLC (Figure S27 vs S24). Then, SPAAC reaction with **9** (ca. 20 equiv) under mildly basic conditions (pH 7.4) afforded Au_{25} cluster-conjugated trastuzumab **13** (Figure 4b). In the second step, basic pH was essential to keep **9** and **13** dissolved by ionizing the carboxylate ligands on the Au_{25} cluster. In SEC-HPLC,[49] the peak absorbing at 380 nm was assigned as Au_{25}-labeled antibody **13**, which had shorter retention time (t_R = 7.40 min) than the parent antibody (mAb, t_R = 7.73 min) (Figures 4d, S21, and S24). A faint band of conjugate could also be observed in SDS-PAGE just above trastuzumab (Figure S21). Protein aggregation was minimal for the optimized 2-step procedure (Figure 4d, lane 3). No evidence of background labeling was found (Figure S29).

We also synthesized Lys-conjugate **14** through condensation of trastuzumab with O-succinimide (N_3-PEG_4-OSu) to produce intermediate **15**,[11] followed by Au_{25} labeling (Figure 4c). The target peak at shorter retention time (t_R = 7.32 min) with strong absorption at 380 nm was observed in SEC-HPLC analysis (Figure 4e and S23), suggesting that the gold content in **14** was higher than in **13**.

Upscaled synthesis, purification, and antigen-binding of Au_{25}-trastuzumab conjugates. Having confirmed bioconjugation of Au_{25} nanocluster to trastuzumab on a small scale at Trp and Lys, we upscaled our experiments to produce modified proteins for further analyses. For purification on a small scale (0.5 mg trastuzumab; 34 μmol), we used columns (10-cm length, 1 g gel) manually filled with Sephadex™-G50. However, we could not separate non-conjugated Au_{25} clusters completely from the conjugates. Longer columns (20-cm length, 2 g gel) performed better, though the separation was still unsatisfactory. Optimal purification results were achieved using an ÄKTA purification system equipped with a Superdex™ 200 Increase 10/300 GL column. We upscaled the Trp- and Lys-selective bioconjugation reactions and the subsequent SPAAC Au_{25} nanocluster labeling reactions using 1 mg proteins (68 μmol), respectively. Conjugates **13** and **14** were successfully separated from the non-modified proteins and excess non-conjugated Au_{25} clusters by ÄKTA purification. The cluster-antibody ratio (CAR) was calculated by UV measurement as 0.66 for **13** and 2.75 for **14** (Figure S66).

We conducted ELISA using purified conjugates **13** and **14** (Figures S62-S64). Binding affinities with HER2 antigen were about 4-times smaller for Trp-conjugate **13** (ED_{50} = 1.65 nM) and about 18 times smaller for Lys-conjugates **14** (EC_{50} = 6.65 nM), than for non-modified trastuzumab (EC_{50}

= 0.37 nM). This is likely due to the fact that the Trp-selective bioconjugation proceeded mainly at the Fc region of the antibody (Figures S31-S48), whereas the Lys-selective bioconjugation occurred randomly over the whole antibody, including the Fab region responsible for antigen recognition. The too-high CAR in **14** could also cause binding suppression. Therefore, advantages of the Trp-selective bioconjugation over the Lys-selective bioconjugation are producing homogeneous conjugates and minimal loss of antigen-binding affinity in antibodies successfully modified with gold clusters.

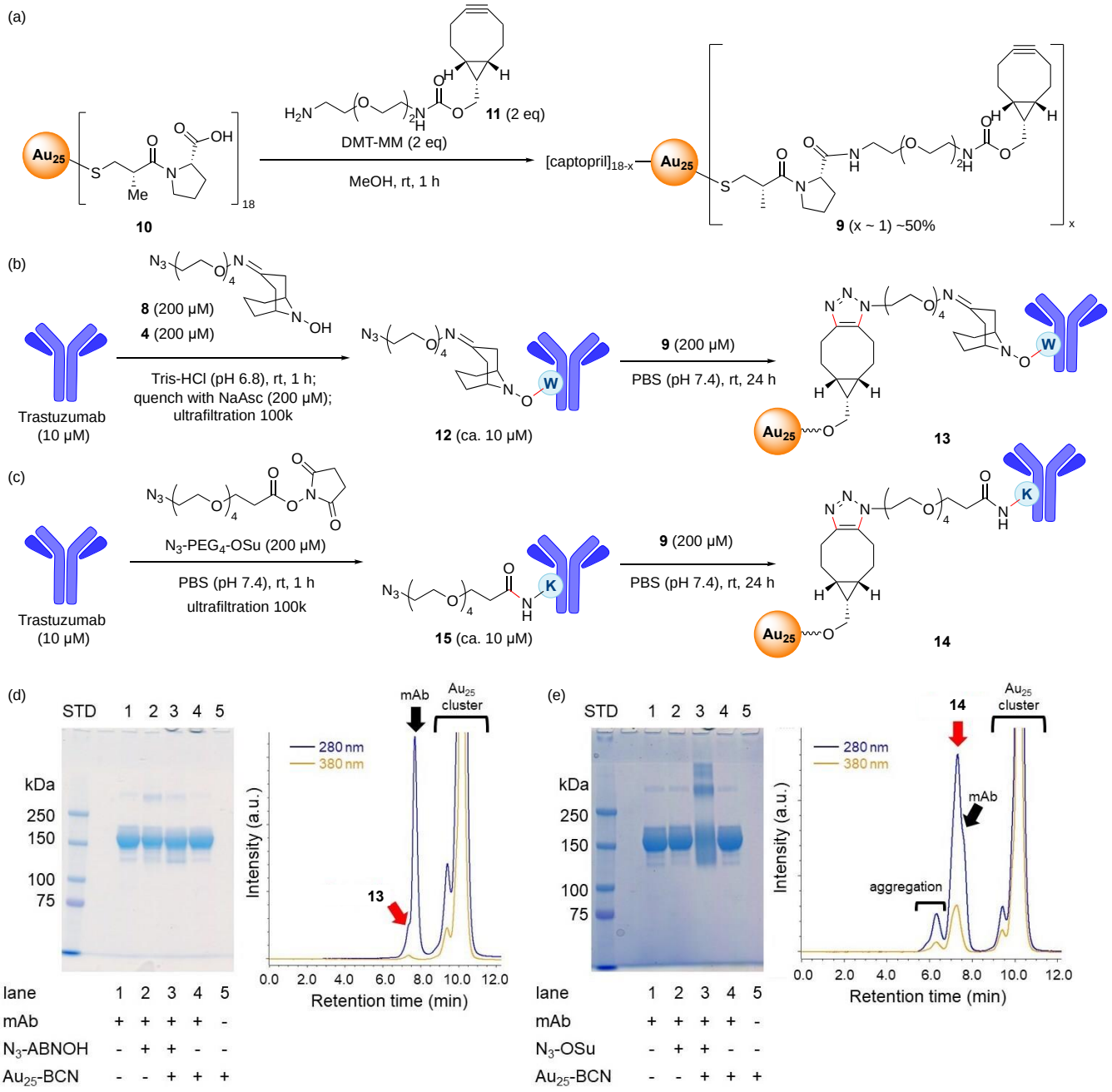

Figure 4. Successful SPAAC strategy for Au_{25} bioconjugation at Trp and Lys. (a) Synthesis of Au_{25}-BCN **9**. (b) SPAAC strategy for Au_{25} bioconjugation at Trp. (c) SPAAC strategy for Au_{25} bioconjugation at Lys. (d) Analysis of Au_{25}-trastuzumab conjugate at Trp **13**. Left: SDS-PAGE. lane 1: trastuzumab only, lane 2: N_3-labeled trastuzumab at Trp (the reaction mixture for generating **12**), lane 3: N_3-labeled trastuzumab at Trp incubated with Au_{25}-BCN **9** (the reaction mixture for generating **13**), lane 4: trastuzumab incubated with Au_{25}-BCN **9**, lane 5: Au_{25}-BCN **9** only. Right: SEC-HPLC of the sample analyzed in SDS-PAGE lane 3. Blue: detection at 280 nm (for proteins). Yellow: detection at 380 nm (for Au clusters). (e) Analysis of Au_{25}-trastuzumab conjugate at Lys **14**. Left: SDS-PAGE. lane 1: trastuzumab only, lane 2: N_3-labeled trastuzumab at Lys (the reaction mixture for generating **15**), lane 3: N_3-labeled trastuzumab at Lys incubated with Au_{25}-BCN **9** (the reaction mixture for generating **14**), lane 4: trastuzumab incubated with Au_{25}-BCN **9**, lane 5: Au_{25}-BCN **9** only. Right: SEC-HPLC of the sample analyzed in SDS-PAGE lane 3. Blue: detection at 280 nm (for proteins). Yellow: detection at 380 nm (for Au clusters).

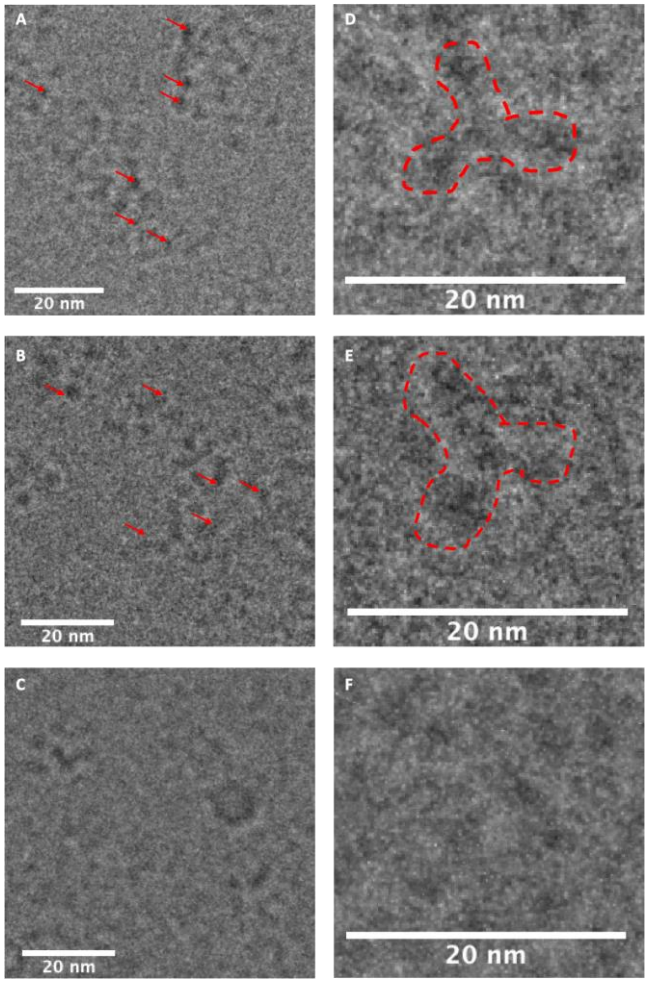

Figure 5. Cryo-EM images of Au_{25} nanocluster-conjugated trastuzumab at Trp (**13**) or Lys (**14**) and unmodified trastuzumab. A, **13**. B, **14**. C, unmodified trastuzumab. Red arrows in A and B indicate Au_{25} nanoclusters. D. A magnified picture of a single particle of **13** (dashed red line). E. A magnified picture of a single particle of **14** (dashed red line). F. A magnified picture of trastuzumab. A single particle was not clearly visible due to the absence of Au clusters. Full images are available in Supporting Information (Figures S71-S73).

Cryo-EM imaging of Au_{25}-trastuzumab conjugates. Samples in adjusted concentrations were first subjected to electron microscopy analysis with negative staining treated by uranyl acetate. Due to the small size of the Au_{25} core and the small difference in electron density between gold and uranium, however, the presence of clusters was not confirmed despite protein being observed. We then proceeded to cryo-EM analysis of freshly synthesized samples and successfully confirmed the presence of gold clusters by applying manual thresholding using ImageJ software (Figures S74-S76). The same threshold value could not be set for micrographs of non-modified trastuzumab due to the lack of intensive diffraction by gold nanoclusters. Standard protein concentrations for cryo-EM analysis should be 1 mg/mL or higher, but we needed to dilute the samples to <0.5 mg/mL to achieve appropriate protein dispersion. The labeled proteins contained small black inclusions corresponding to Au_{25} clusters (see red arrows in Figures 5A and B). More of these inclusions were observed in images for Lys-conjugate **14** than Trp-conjugate **13**. This observation is consistent with the SEC-HPLC results and CAR calculations (Figure S66). Single particle analysis based on acquired micrographs has not been successful so far, likely due to the relatively small size and high flexibility of the antibody.

DISCUSSION

Structurally well-defined Au_{25} nanocluster is a promising electron probe for cryo-EM and -ET due to its small size, stability against aggregation, and simplicity in ligand modifications, synthesis, and purification. Here we have demonstrated for the first time that Au_{25} nanocluster can be conjugated with an antibody through Trp-selective bioconjugation. Due to the broad scope of click chemistry, intermediate **12** will be a versatile hub compound for homogenous protein modifications, not limited to immunogold synthesis. The coupling partner **9**, an Au_{25} nanocluster presenting an alkyne handle, is also noteworthy for several reasons. First, the degree of amide formation (x in Figure 4a) on the Au_{25} nanocluster was controlled to approximately 1 by tuning the stoichiometry between **10** and **11**. This is critical in avoiding protein aggregation by SPAAC bridging plural proteins through multivalent covalent bond-formation with **9**. Second, **9** was compatible with aqueous, mildly basic buffer despite possessing a hydrophobic BCN moiety. Nevertheless, yield of SPAAC between **9** and **12** was low to moderate, though the same reaction between **9** and **15** proceeded in high yield. The reason for this contrasting reactivity between **12** and **15** might be due to the higher number of Lys residues available for SPAAC in comparison to Trp residues, which are relatively rare and buried within protein. Systematic studies upon linker structures between the keto-ABNO and azide moieties will be necessary to improve the conjugation efficiency. It was reported that short and less-flexible linkers between the gold nanocluster and protein are beneficial for high-resolution cryo-EM probes[4,20,23]. Therefore, future optimization studies should focus on improvements applicable to shorter linkers.

Evaluation of the Trp-conjugated Au_{25} immunogold function and utility as an electron probe for cryo-EM and -ET in structural biology studies is the next important step. The utility of homogenous Au_{25} nanocluster-conjugated antibodies will not be limited to electron probes, however. Since Au nanoclusters exhibit interesting optical properties such as absorption/emission of near-infrared light and photo-induced generation of active oxygen species,[50] their protein conjugates can also be applied as photo or radiosensitizers for creating potential new anti-cancer therapies.[51,52]

CONCLUSION

We achieved the first bioconjugation of sub-nanometer-size Au_{25} clusters to an antibody at Trp without protein engineering. To minimize potential damage to the sensitive

protein and payload, we developed a new protocol for Trp-selective bioconjugation using keto-ABNOH (**3**, **7**, and **8**) and isolated TEMPO$^+$ **4** in a neutral pH buffer. This improved two-step procedure for Trp-selective bioconjugation, along with SPAAC, produced the antibody-Au_{25} nanocluster conjugate effectively. The conjugate was functional, retaining a reasonable antigen binding affinity. Furthermore, its function as an electron probe was confirmed by cryo-EM studies. The results presented here will aid in developing a novel electron probe for immunogold labeling with an improved signal-to-noise ratio and facilitating cryo-EM and -ET analysis for complicated biological events.

ASSOCIATED CONTENT

Supporting Information

The Supporting Information is available free of charge on the ACS Publications website.
Detailed experimental conditions and methods, Figure S1–S76, and NMR charts of new compounds (PDF)

AUTHOR INFORMATION

Corresponding Authors

Kounosuke Oisaki† – Graduate School of Pharmaceutical Sciences, The University of Tokyo, 7-3-1 Hongo, Bunkyo-ku, Tokyo 113-0033, Japan; orcid.org/0000-0002-0499-8168; Email: oisaki@g.ecc.u-tokyo.ac.jp
Motomu Kanai – Graduate School of Pharmaceutical Sciences, The University of Tokyo, 7-3-1 Hongo, Bunkyo-ku, Tokyo 113-0033, Japan; orcid.org/0000-0003-1977-7648; Email: kanai@mol.f.u-tokyo.ac.jp

Authors

Katarzyna Joanna Malawska – Graduate School of Pharmaceutical Sciences, The University of Tokyo, Bunkyo-ku, Tokyo 113-0033, Japan

Shinjiro Takano – Graduate School of Science, The University of Tokyo, Bunkyo-ku, Tokyo 113-0033, Japan; orcid.org/0000-0001-9262-5283.

Haruaki Yanagisawa – Graduate School of Medicine, The University of Tokyo, Bunkyo-ku, Tokyo 113-0033, Japan; https://orcid.org/0000-0003-0313-2343.

Tatsuya Tsukuda – Graduate School of Science, The University of Tokyo, Bunkyo-ku, Tokyo 113-0033, Japan; orcid.org/0000-0002-0190-6379.

Masahide Kikkawa – Graduate School of Medicine, The University of Tokyo, Bunkyo-ku, Tokyo 113-0033, Japan; https://orcid.org/0000-0001-7656-8194.

Present Address

†Interdisciplinary Research Center for Catalytic Chemistry (IRC3), National Institute of Advanced Industrial Science and Technology (AIST), Tsukuba Central 5-2, 1-1-1 Higashi, Tsukuba, Ibaraki 305-8565, Japan; Email: k.oisaki@aist.go.jp

Author Contributions

The manuscript was written through the contributions of all authors. / All authors have given approval to the final version of the manuscript.

Funding Sources

This work was supported in part by JSPS KAKENHI Grant Numbers JP20K21472 (for M. Kanai), JP21H05077 (for K. O.), and JP20H00370 (for T. T.), and JST-CREST Grant No. JPMJCR20B2 (for T. T.). K. J. M. would like to thank for the MEXT scholarship. We also acknowledge the Platform Project for Supporting Drug Discovery and Life Science Research (Basis for Supporting Innovative Drug Discovery and Life Science Research (BINDS)) from the Japan Agency for Medical Research and Development (AMED) under grant numbers 22ama121002j0001 (to M. Kikkawa).

ACKNOWLEDGMENT

The authors would like to sincerely thank Prof. H. Häkkinen, Prof. V. Marjomäki (University of Jyväskylä), and Dr. M. Stark (Astellas Gene Therapies) for their kind advice on separation of gold cluster conjugates. We acknowledge Dr. Kazuhiko Nakamura, Yoichi Sakamaki, and Toshie Furuya for their assistance with cryo-EM measurement and analysis, and Yuki Kobayashi for her technical assistance in purification and analysis of the conjugates. We thank R. Newlon (Univ. Tokyo) for reading the manuscript and providing helpful comments.

ABBREVIATIONS

ABNO, 9-Azabicyclo[3.3.1]nonane *N*-oxyl; ABNOH, 9-Azabicyclo[3.3.1]nonan-9-ol; BCN, Bicyclo[6.1.0]nonyne; CBB, Coomassie brilliant blue; DMT-MM, 4-(4,6-Dimethoxy-l,3,5-triazin-2-yl)-4-methylmorpholinium chloride; EC_{50}; half maximal effective concentration; ELISA, enzyme linked immunosorbent assay; Fab, fragment antigen-binding; FITC; fluorescein isothiocyanate; HER2, human epidermal growth factor 2; His, histidine; HPLC, high-performance liquid chromatography; mAB, monoclonal antibody; mM, millimolar; μM, micromolar; nM, nanomolar; nm, nanometer; NMR, nuclear magnetic resonance; PBS, phosphate buffered saline; pH, potential of hydrogen; Phe, phenylalanine; rt, room temperature; scFv, single chain fragment variable; Ser, serine; SDS-PAGE, sodium dodecyl sulphate polyacrylamide gel electrophoresis; SEC, size exclusion chromatography; TEMPO, 2,2,6,6-tetramethylpiperidine 1-oxyl radical; TEMPO$^+$, 2,2,6,6-tetramethyl-1-oxopiperidinium tetrafluoroborate; Tris HCl, tris(hydroxymethyl)aminomethane hydrochloride; Tyr, tyrosine;

REFERENCES

(1) Thompson, R. F.; Walker, M.; Siebert, C. A.; Muench, S. P.; Ranson, N. A. An Introduction to Sample Preparation and Imaging by Cryo-Electron Microscopy for Structural Biology. *Methods* **2016**, *100* (2016), 3–15. https://doi.org/10.1016/j.ymeth.2016.02.017.

(2) Renaud, J. P.; Chari, A.; Ciferri, C.; Liu, W. T.; Rémigy, H. W.; Stark, H.; Wiesmann, C. Cryo-EM in Drug Discovery: Achievements, Limitations and Prospects. *Nat. Rev. Drug Discov.* **2018**, *17* (7), 471–

492. https://doi.org/10.1038/nrd.2018.77.

(3) D'Imprima, E.; Kühlbrandt, W. Current Limitations to High-Resolution Structure Determination by Single-Particle CryoEM. *Q. Rev. Biophys.* **2021**. https://doi.org/10.1017/S0033583521000020.

(4) Ackerson, C. J.; Powell, R. D.; Hainfeld, J. F. Site-Specific Biomolecule Labeling with Gold Clusters. In *Methods in Enzymology*; Academic Press Inc., 2010; Vol. 481, pp 195–230. https://doi.org/10.1016/S0076-6879(10)81009-2.

(5) Faulk, P. W.; Taylor, M. G. An Immunocoloid Method for the Electron Microscope. *Immunochemistry* **1971**, *8* (March), 1081–1083.

(6) Hainfeld, J. F.; Powell, R. D. New Frontiers in Gold Labeling. *J. Histochem. Cytochem.* **2000**, *48* (4), 471–480. https://doi.org/10.1177/002215540004800404.

(7) Daniel, M. C.; Astruc, D. Gold Nanoparticles: Assembly, Supramolecular Chemistry, Quantum-Size-Related Properties, and Applications Toward Biology, Catalysis, and Nanotechnology. *Chem. Rev.* **2004**, *104* (1), 293–346. https://doi.org/10.1021/cr030698+.

(8) Ochtrop, P.; Hackenberger, C. P. R. Recent Advances of Thiol-Selective Bioconjugation Reactions. *Curr. Opin. Chem. Biol.* **2020**, *58*, 28–36. https://doi.org/10.1016/j.cbpa.2020.04.017.

(9) Broadwith, P. No Title https://www.chemistryworld.com/news/explainer-what-is-cryo-electron-microscopy/3008091.article (accessed Jun 29, 2022).

(10) Matikonda, S. S.; Mclaughlin, R.; Shrestha, P.; Lipshultz, C.; Schnermann, M. J. Structure-Activity Relationships of Antibody-Drug Conjugates: A Systematic Review of Chemistry on the Trastuzumab Scaffold. *Bioconjug. Chem.* **2022**. https://doi.org/10.1021/acs.bioconjchem.2c00177.

(11) Haque, M.; Forte, N.; Baker, J. R. Site-Selective Lysine Conjugation Methods and Applications towards Antibody-Drug Conjugates. *Chem. Commun.* **2021**, *57* (82), 10689–10702. https://doi.org/10.1039/d1cc03976h.

(12) Ramsey, A. V.; Bischoff, A. J.; Francis, M. B. Enzyme Activated Gold Nanoparticles for Versatile Site-Selective Bioconjugation. *J. Am. Chem. Soc.* **2021**, *143* (19), 7342–7350. https://doi.org/10.1021/jacs.0c11678.

(13) Hainfeld, J. F. Labeling with Nanogold and Undecagold: Techniques and Results. *Scanning Microsc. Suppl.* **1996**, *10* (10).

(14) Bartiett, P. A.; Bauer, B.; Sanger, S. J. Synthesis of Water-Soluble Uridecagold Cluster Compounds of Potential Importance in Electron Microscopic and Other Studies of Biological Systems. *J. Am. Chem. Soc.* **1978**, *100* (16), 5085–5089. https://doi.org/10.1021/ja00484a029.

(15) Hainfeld, J. F. A Small Gold-Conjugated Antibody Label: Improved Resolution for Electron Microscopy. *Science (80-.).* **1987**, *236* (4800), 450–453. https://doi.org/10.1126/science.3563522.

(16) Milligan, R. A.; Whittaker, M.; Safer, D. Molecular Structure of F-Actin and Location of Surface Binding Sites. *Nature* **1990**, *348* (6298), 217–221. https://doi.org/10.1038/348217a0.

(17) Lipka, J. J.; Hainfeld, J. F.; Wall, J. S. Undecagold Labeling of a Glycoprotein: STEM Visualization of an Undecagoldphosphine Cluster Labeling the Carbohydrate Sites of Human Haptoglobin-Hemoglobin Complex. *J. Ultrasructure Res.* **1983**, *84* (2), 120–129. https://doi.org/10.1016/S0022-5320(83)90123-5.

(18) Crum, J.; Gruys, K. J.; Frey, T. G. Electron Microscopy of Cytochrome c Oxidase Crystals: Labeling of Subunit III with a Monomaleimide Undecagold Cluster Compound. *Biochemistry* **1994**, *33* (46), 13719–13726. https://doi.org/10.1021/bi00250a024.

(19) Kikkawa, M.; Okada, Y.; Hirokawa, N. 15 Å Resolution Model of the Monomeric Kinesin Motor, KIF1A. *Cell* **2000**, *100* (2), 241–252. https://doi.org/10.1016/S0092-8674(00)81562-7.

(20) Ackerson, C. J.; Jadzinsky, P. D.; Jensen, G. J.; Kornberg, R. D. Rigid, Specific, and Discrete Gold Nanoparticle/Antibody Conjugates. *J. Am. Chem. Soc.* **2006**, *128* (8), 2635–2640. https://doi.org/10.1021/ja0555668.

(21) Ackerson, C. J.; Jadzinsky, P. D.; Sexton, J. Z.; Bushnell, D. A.; Kornberg, R. D. Synthesis and Bioconjugation of 2 and 3 Nm-Diameter Gold Nanoparticles. *Bioconjug. Chem.* **2010**, *21* (2), 214–218. https://doi.org/10.1021/bc900135d.

(22) Levi-Kalisman, Y.; Jadzinsky, P. D.; Kalisman, N.; Tsunoyama, H.; Tsukuda, T.; Bushnell, D. A.; Kornberg, R. D. Synthesis and Characterization of Au 102 (p -MBA) 44 Nanoparticles. **2011**, *133*,

2976–2982.

(23) Stark, M. C.; Baikoghli, M. A.; Lahtinen, T.; Malola, S.; Xing, L.; Nguyen, M.; Nguyen, M.; Sikaroudi, A.; Marjomäki, V.; Häkkinen, H.; Cheng, R. H. Structural Characterization of Site-Modified Nanocapsid with Monodispersed Gold Clusters. *Sci. Rep.* **2017**, *7*. https://doi.org/10.1038/s41598-017-17171-x.

(24) Marjomäki, V.; Lahtinen, T.; Martikainen, M.; Koivisto, J.; Malola, S.; Salorinne, K.; Pettersson, M.; Häkkinen, H. Site-Specific Targeting of Enterovirus Capsid by Functionalized Monodisperse Gold Nanoclusters. *Proc. Natl. Acad. Sci. U. S. A.* **2014**, *111* (4), 1277–1281. https://doi.org/10.1073/pnas.1310973111.

(25) Kang, X.; Chong, H.; Zhu, M. Au25(SR)18: The Captain of the Great Nanocluster Ship. *Nanoscale* **2018**, *10* (23), 10758–10834. https://doi.org/10.1039/c8nr02973c.

(26) Dahan, I.; Sorrentino, S.; Boujemaa-Paterski, R.; Medalia, O. Tiopronin-Protected Gold Nanoparticles as a Potential Marker for Cryo-EM and Tomography. *Structure* **2018**, *26* (10), 1408-1413.e3. https://doi.org/10.1016/j.str.2018.06.009.

(27) Yuan, X.; Yu, Y.; Yao, Q.; Zhang, Q.; Xie, J. Fast Synthesis of Thiolated Au 25 Nanoclusters via Protection-Deprotection Method. *J. Phys. Chem. Lett.* **2012**, *3* (17), 2310–2314. https://doi.org/10.1021/jz300960b.

(28) Negishi, Y.; Nobusada, K.; Tsukuda, T. Glutathione-Protected Gold Clusters Revisited: Bridging the Gap between Gold(I)-Thiolate Complexes and Thiolate-Protected Gold Nanocrystals. *J. Am. Chem. Soc.* **2005**, *127* (14), 5261–5270. https://doi.org/10.1021/ja042218h.

(29) Xie, J.; Zheng, Y.; Ying, J. Y. Protein-Directed Synthesis of Highly Fluorescent Gold Nanoclusters. *J. Am. Chem. Soc.* **2009**, *131* (3), 888–889. https://doi.org/10.1021/ja806804u.

(30) Takahata, R.; Yamazoe, S.; Maehara, Y.; Yamazaki, K.; Takano, S.; Kurashige, W.; Negishi, Y.; Gohara, K.; Tsukuda, T. Electron Microscopic Observation of an Icosahedral Au13 Core in Au25(SePh)18 and Reversible Isomerization between Icosahedral and Face-Centered Cubic Cores in Au144(SC2H4Ph)60. *J. Phys. Chem. C* **2020**, *124* (12), 6907–6912. https://doi.org/10.1021/acs.jpcc.9b11412.

(31) Rojas-Cervellera, V.; Raich, L.; Akola, J.; Rovira, C. The Molecular Mechanism of the Ligand Exchange Reaction of an Antibody against a Glutathione-Coated Gold Cluster. *Nanoscale* **2017**, *9* (9), 3121–3127. https://doi.org/10.1039/c6nr08498b.

(32) Moelbert, S.; Emberly, E.; Tang, C. Correlation between Sequence Hydrophobicity and Surface-Exposure Pattern of Database Proteins. *Protein Sci.* **2004**, *13* (3), 752–762. https://doi.org/10.1110/ps.03431704.

(33) Gilis, D.; Massar, S.; Cerf, N. J.; Rooman, M. Optimality of the Genetic Code with Respect to Protein Stability and Amino-Acid Frequencies. *Genome Biol.* **2001**, *2* (11), 1–12. https://doi.org/10.1186/gb-2001-2-11-research0049.

(34) Seki, Y.; Ishiyama, T.; Sasaki, D.; Abe, J.; Sohma, Y.; Oisaki, K.; Kanai, M. Transition Metal-Free Tryptophan-Selective Bioconjugation of Proteins. *J. Am. Chem. Soc.* **2016**, *138* (34), 10798–10801. https://doi.org/10.1021/jacs.6b06692.

(35) Maruyama, K.; Malawska, K. J.; Konoue, N.; Oisaki, K.; Kanai, M. Synthesis of Tryptophan-Folate Conjugates. *Synlett* **2020**, *31* (8), 784–787. https://doi.org/10.1055/s-0039-1691735.

(36) Tagawa, H.; Maruyama, K.; Sasaki, K.; Konoue, N.; Kishimura, A.; Kanai, M.; Mori, T.; Oisaki, K.; Katayama, Y. Induction of ADCC by a Folic Acid-MAb Conjugate Prepared by Tryptophan-Selective Reaction toward Folate-Receptor-Positive Cancer Cells. *RSC Adv.* **2020**, *10* (28), 16727–16731. https://doi.org/10.1039/dora03291c.

(37) Toyama, E.; Maruyama, K.; Sugai, T.; Kondo, M.; Masaoka, S. Electrochemical Tryptophan-Selective Bioconjugation. *ChemRxiv* **2019**. https://doi.org/doi: 10.26434/chemrxiv.7795484.v.

(38) Mercadante, M. A.; Kelly, C. B.; Bobbitt, J. M.; Tilley, L. J.; Leadbeater, N. E. Synthesis of 4-Acetamido-2,2,6,6-Tetramethylpiperidine-1-Oxoammonium Tetrafluoroborate and 4-Acetamido-(2,2,6,6-Tetramethyl-Piperidin-1-Yl)Oxyl and Their Use in Oxidative Reactions. *Nat. Protoc.* **2013**, *8* (4), 666–676. https://doi.org/10.1038/nprot.2013.028.

(39) Bobbitt, J. M. Oxoammonium Salts. 6. 4-Acetylamino-2,2,6,6-Tetramethylpiperidine-1-Oxoammonium Perchlorate: A Stable and Convenient Reagent for the Oxidation of Alcohols. Silica Gel Catalysis. *J. Org. Chem.* **1998**, *63* (25), 9367–9374. https://doi.org/10.1021/jo981322c.

(40) Hostetler, M. J.; Templeton, A. C.; Murray, R. W. Dynamics of Place-Exchange Reactions on Monolayer-Protected Gold Cluster Molecules. *Langmuir* **1999**, *15* (11), 3782–3789. https://doi.org/10.1021/la981598f.

(41) Salassa, G.; Sels, A.; Mancin, F.; Bürgi, T. Dynamic Nature of Thiolate Monolayer in Au25(SR)18 Nanoclusters. *ACS Nano* **2017**, *11* (12), 12609–12614. https://doi.org/10.1021/acsnano.7b06999.

(42) Klán, P.; Šolomek, T.; Bochet, C. G.; Blanc, A.; Givens, R.; Rubina, M.; Popik, V.; Kostikov, A.; Wirz, J. Photoremovable Protecting Groups in Chemistry and Biology: Reaction Mechanisms and Efficacy. *Chem. Rev.* **2013**, *113* (1), 119–191. https://doi.org/10.1021/cr300177k.

(43) Weinstain, R.; Slanina, T.; Kand, D.; Klán, P. Visible-to-NIR-Light Activated Release: From Small Molecules to Nanomaterials. *Chem. Rev.* **2020**, *120* (24), 13135–13272. https://doi.org/10.1021/acs.chemrev.0c00663.

(44) Givens, R. S.; Rubina, M.; Wirz, J. Applications of P-Hydroxyphenacyl (PHP) and Coumarin-4-Ylmethyl Photoremovable Protecting Groups. *Photochem. Photobiol. Sci.* **2012**, *11* (3), 472–488. https://doi.org/10.1039/c2pp05399c.

(45) Agard, N. J.; Prescher, J. A.; Bertozzi, C. R. A Strain-Promoted [3 + 2] Azide-Alkyne Cycloaddition for Covalent Modification of Biomolecules in Living Systems. *J. Am. Chem. Soc.* **2004**, *126* (46), 15046–15047. https://doi.org/10.1021/ja044996f.

(46) Pickens, C. J.; Johnson, S. N.; Pressnall, M. M.; Leon, M. A.; Berkland, C. J. Practical Considerations, Challenges, and Limitations of Bioconjugation via Azide-Alkyne Cycloaddition. *Bioconjug. Chem.* **2018**, *29* (3), 686–701. https://doi.org/10.1021/acs.bioconjchem.7b00633.

(47) Choi, J.; Fields-zinna, C. A.; Stiles, R. L.; Balasubramanian, R.; Douglas, A. D.; Crowe, M. C.; Murray, R. W. Reactivity of [Au25(SCH2CH2Ph)18]1- Nanoparticles with Metal Ions. *J. Phys. Chem. C* **2010**, *114*, 15890–15896.

(48) Waszkielewicz, M.; Olesiak-Banska, J.; Comby-Zerbino, C.; Bertorelle, F.; Dagany, X.; Bansal, A. K.; Sajjad, M. T.; Samuel, I. D. W.; Sanader, Z.; Rozycka, M.; Wojtas, M.; Matczyszyn, K.; Bonacic-Koutecky, V.; Antoine, R.; Ozyhar, A.; Samoc, M. PH-Induced Transformation of Ligated Au25 to Brighter Au23 Nanoclusters. *Nanoscale* **2018**, *10* (24), 11335–11341. https://doi.org/10.1039/c8nr00660a.

(49) Matsuda, Y. Current Approaches for the Purification of Antibody–Drug Conjugates. *J. Sep. Sci.* **2022**, *45* (1), 27–37. https://doi.org/10.1002/jssc.202100575.

(50) Kawasaki, H.; Kumar, S.; Li, G.; Zeng, C.; Kauffman, D. R.; Yoshimoto, J.; Iwasaki, Y.; Jin, R. Generation of Singlet Oxygen by Photoexcited Au25(SR) 18 Clusters. *Chem. Mater.* **2014**, *26* (9), 2777–2788. https://doi.org/10.1021/cm500260z.

(51) Zhang, X. D.; Chen, J.; Luo, Z.; Wu, D.; Shen, X.; Song, S. S.; Sun, Y. M.; Liu, P. X.; Zhao, J.; Huo, S.; Fan, S.; Fan, F.; Liang, X. J.; Xie, J. Enhanced Tumor Accumulation of Sub-2 Nm Gold Nanoclusters for Cancer Radiation Therapy. *Adv. Healthc. Mater.* **2014**, *3* (1), 133–141. https://doi.org/10.1002/adhm.201300189.

(52) Katla, S. K.; Zhang, J.; Castro, E.; Bernal, R. A.; Li, X. Atomically Precise Au25(SG)18 Nanoclusters: Rapid Single-Step Synthesis and Application in Photothermal Therapy. *ACS Appl. Mater. Interfaces* **2018**, *10* (1), 75–82. https://doi.org/10.1021/acsami.7b12614.

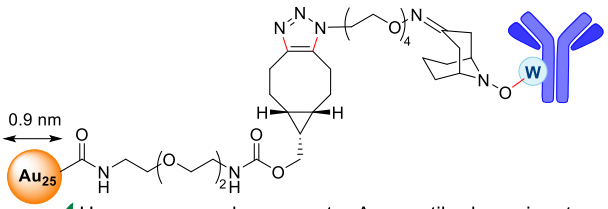

- Homogenous sub-nanometer Au_{25}-antibody conjugate
- Promising immunogold labeling reagent